

Giant Nernst Effect and Lock-In Currents at Magic Angles in $(\text{TMTSF})_2\text{PF}_6$

W. Wu,* I. J. Lee,† and P. M. Chaikin

Department of Physics, Princeton University, Princeton, New Jersey, 08544, USA
(Received 26 February 2003; published 28 July 2003)

We have measured the thermoelectric signal along the \mathbf{a} axis in $(\text{TMTSF})_2\text{PF}_6$ at 10 kbar as a function of the orientation of the applied magnetic field. Resonantlike Nernst signals were found with a dramatic sign change as the field was rotated through the “Lebed magic angles.” The sign change indicates that the electrical current is “locked in” to the magic angle (interchain) directions for field alignment close to, but on either side of, the magic angles. The amplitude of signals near these angles is many orders of magnitude larger than expected from conventional Boltzmann transport theory.

DOI: 10.1103/PhysRevLett.91.056601

PACS numbers: 72.15.Nj, 72.15.Gd, 72.15.Jf, 75.30.Fv

$(\text{TMTSF})_2\text{PF}_6$, the first organic superconductor [1], is quite an unusual material. It is metallic, semiconducting, insulating, superconducting, antiferromagnetic, spin and charge density wave, and exhibits a cascade of first-order field-induced spin density wave (FISDW) transitions, with a bulk three-dimensional quantum Hall effect, as temperature, pressure, and magnetic field are varied [2]. Recent studies suggest it is a triplet superconductor [3] and non-Fermi liquid [4,5]. There are also striking angular-dependent effects with large dips in the magnetoresistance at “magic angles” (MA) [6], which correspond to commensurate \mathbf{k} space orbits [7]. $(\text{TMTSF})_2\text{PF}_6$ is a highly anisotropic conductor consisting of chains of TMTSF molecules (bandwidth ~ 1 eV) along \mathbf{a} coupled to neighboring chains (bandwidth ~ 0.1 eV) along \mathbf{b} to form conducting planes. The interplane coupling (~ 0.003 eV) along \mathbf{c} is weakest. The MA effects occur when the magnetic field is aligned in the direction between chains [8]. The effects have been attributed to Fermi surface features, dimensional crossovers, or interplane decoupling. Although there are many theories and models for the MA effects [9–11], none of them satisfactorily explain the experiments. Studies of the temperature dependence of the magnetoresistance of $(\text{TMTSF})_2\text{PF}_6$ [12] suggest angular-dependent electronic ground state, i.e., metallic at the MAs and non-metallic at other orientations as the temperature is lowered. If the electronic ground state of $(\text{TMTSF})_2\text{PF}_6$ is determined by the orientation of the magnetic field, it will be reflected in the thermoelectric power (TEP). Therefore, we carried out a thermoelectric study of $(\text{TMTSF})_2\text{PF}_6$ under 10 kbar of pressure where the MA effects are clearly evident in conductivity measurements.

The thermoelectric measurements revealed several striking and unusual features. The measured voltage is predominantly odd in magnetic field, indicating a Nernst rather than Seebeck (TEP) effect. There are pronounced features near the Lebed MAs: an increase in thermoelectric voltage as the field is rotated toward the MA, a maximum preceding and then a fall to zero at the MA,

and approximately antisymmetric behavior as the field rotation is continued away from the MA. The magnitude of the thermoelectric voltage, $\sim 10 \mu\text{V}/\text{K}$ at 0.2 K, 7.5 T near the maxima or minima, is enormous compared to values measured for any other material measured to date. Conventional Fermi liquids exhibit thermoelectric voltages ~ 1 nV/K under similar conditions. The resonantlike structures strongly indicate that at and near field alignment with an interchain direction (MA) the quasiparticle current flows directly in the interchain direction. As field is rotated toward another interchain direction, the current shifts toward lock-in with that interchain direction. The giant value to the thermoelectric voltage may result from strong correlations or a metal-insulator transition as a function of field direction.

The schematic in the inset of Fig. 1 shows the experimental setup inside the pressure clamp and follows previous thermopower techniques prescribed for pressure [13]. The heat flow is primarily through the frozen pressure fluid from the heater to the base and walls. The temperature profile is complex. The temperature gradient used was 50–100 mK at low temperature. A low frequency switching dc technique was used to turn the heater on and off for signal averaging [14]. The magnetoresistance was measured along with the thermoelectric voltages. The pressure cell was attached to the mixing chamber of a dilution refrigerator and the entire cryostat was rotated by a goniometer. The sample was sitting at the center of a superconducting split-coil magnet so that the magnetic field was rotated in the $\mathbf{b}^*\mathbf{c}^*$ plane ($\perp \mathbf{a}$ axis).

The temperature gradient established by the pressure fluid is not necessarily along the \mathbf{a} axis of sample; a small transverse temperature gradient is possible. The thermoelectric voltage has contributions from both the Seebeck effect (TEP) and the Nernst effect. In the absence of time reversal or inversion symmetry breaking we expect the TEP $S_{aa} \equiv \Delta V_a / \Delta T_a$ to be an even function of magnetic field \mathbf{B} , while the Nernst effect $N_{ac} \equiv \Delta V_a / \Delta T_c$ is an odd function of \mathbf{B} . This can be understood by analog with the longitudinal resistance (even) and Hall resistance (odd),

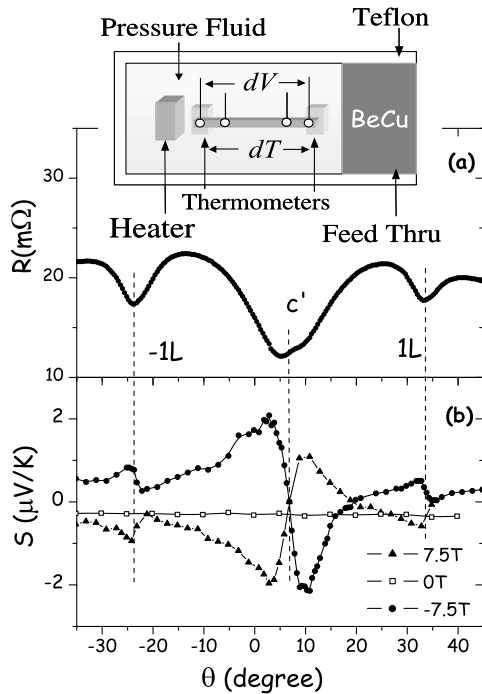


FIG. 1. The experiment setup. (Inset): Four Au wires were attached to the sample along the \mathbf{a} axis. Two RuO thin film resistors thermometers were placed next to both ends of the sample to measure temperature gradient generated by a miniature heater. The angular dependence of the magnetoresistance (a) and the raw thermoelectric signal (b), $S = \Delta V / \Delta T$, for $(\text{TMTSF})_2\text{PF}_6$ as a function of magnetic field direction for $\mathbf{b}^* \mathbf{c}^*$ plane rotation (2 K, 10 kbar). $\theta = 0$ is taken as $\mathbf{B} \parallel \mathbf{c}^*$. Note that S is essentially an odd function of applied field. The solid line is a guide to the eye.

which are even and odd from their Onsager relations [15]. We follow the definition that *Seebeck signal is an even function of magnetic field; Nernst signal is an odd function of magnetic field*. We apply this definition to interpret our data.

The magnetoresistance of our sample at 7.5 T, 2 K, for a field rotation from -35° to 45° is shown in Fig. 1(a). The sharp dips in the magnetoresistance are identified with “Lebed MAs” at $0L = 7^\circ$ (\mathbf{c}'), $1L = 33^\circ$, $-1L = -24^\circ$, corresponding to the real space interchain vectors \mathbf{c}' , $\mathbf{b}' + \mathbf{c}'$, and $-\mathbf{b}' + \mathbf{c}'$. The thermoelectric signal as a function of applied field angle is shown in Fig. 1(b) for 7.5, 0, and -7.5 T. At $B = 0$ the signal seems to be dominated by the contribution of the Au leads, a contribution which is suppressed by the application of a field of ~ 1 T. At 7.5 T the thermoelectric voltage is essentially an odd function of \mathbf{B} , hence dominated by the Nernst rather than Seebeck (TEP) effect, according to our definition. To our experimental uncertainty $S < 0.2 \mu\text{V/K}$ for $T < 2$ K, in agreement with previous reports [16]. However, the Nernst effect is surprisingly large with pronounced structure in the vicinity of the Lebed MAs.

These results were sufficiently surprising that we performed a series of tests to determine whether they were experimental artifacts. First, we tested for linear response. We increased the temperature gradient from 45 to 90 mK and found that the thermoelectric voltage also doubled, as expected for a thermoelectric signal. Second, we changed the heater current source from dc to ac to eliminate the possibility of dc coupling between the heater and sample leads. The thermoelectric voltage depended only on the heater power. Third, we changed rotation direction and did not find any correlation between rotation direction and the thermoelectric voltage (noting that the thermal voltage resembles the derivative of the magnetoresistance with respect to angle). Finally, we rotated the sample at zero field and got the same thermoelectric voltage for all angles [see Fig. 1(b)]. In all, we confirmed that the thermoelectric voltage comes from the sample, is linear with temperature gradient and odd with respect to the magnetic field, and therefore is related to the Nernst effect. Our experimental setup was designed for a longitudinal thermoelectric measurement. So, in terms of geometry, the signal should have been dominated by a Seebeck signal. However, a transverse temperature gradient can exist in the pressure cell, and this temperature gradient can generate a Nernst signal along the \mathbf{a} axis. In our case it appears that the Nernst signal is exceptionally large, and the Seebeck signal is negligible, even though the longitudinal temperature gradient is probably bigger than the transverse one. Because of the unknown locations of the isotherms and limited number of thermometers, we estimate the transverse temperature gradient ΔT_\perp [17], which generates the thermoelectric voltage along \mathbf{a} through the Nernst coefficient N (or N_{ac}), with the temperature gradient along \mathbf{a} , ΔT_\parallel , the biggest ΔT inside the pressure cell. Thus, the angular, field, and temperature dependencies of N are well defined, but the absolute value is a lower limit.

In Fig. 2 we show the angular dependence of the Nernst signal at 2, 1, and 0.2 K with $B = 7.5$ T. There are resonantlike features at the MAs when the sample is in the “normal” metallic state. At 1 K the maximum peak-to-peak (PP) is about $10 \mu\text{V/K}$ at \mathbf{c}' . The PP value at $\pm 1L$ is about $3\text{--}4 \mu\text{V/K}$. A tiny wiggle at $-2L$ (-42°) indicates that similar features may exist for higher order MAs with much smaller amplitudes. As long as the sample remains in the “metallic” state, the Nernst signal increases with decreasing temperature. Note, however, that the structure around \mathbf{c}' has disappeared in the 0.2 K data. At 0.2 K, $(\text{TMTSF})_2\text{PF}_6$ goes into the FISDW state when the magnetic field component along the \mathbf{c}^* axis $B_z > 5$ T (from magnetoresistance measurements of this sample). At 7.5 T, the sample was far into the FISDW state for $\mathbf{B} \parallel \mathbf{c}'$, while it just entered the FISDW for $\mathbf{B} \parallel \pm 1L$. Our temperature dependence studies indicate that the Nernst resonances decrease rapidly on entering the FISDW state.

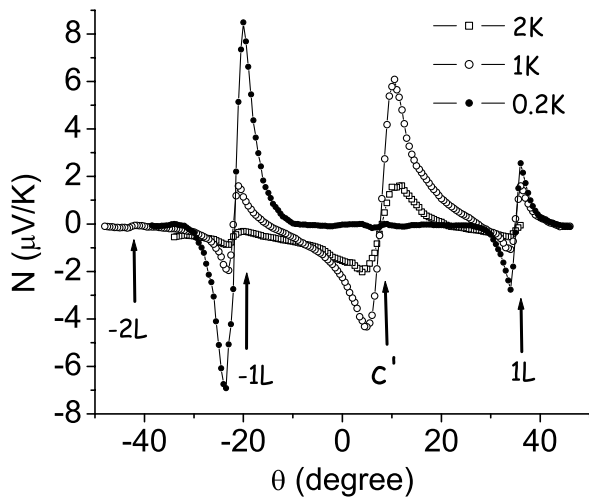


FIG. 2. Angular dependence of the Nernst signal at 2, 1, and 0.2 K, $B = 7.5$ T showing the rapid growth with lower temperature. We have used $N = \frac{S(B) - S(-B)}{2}$ as our definition for the Nernst signal.

The Nernst signals for most conventional metals is linear with magnetic field. In Fig. 3 we show the field dependence of the peak-to-peak Nernst resonance for c' at 2 and 1 K and for $-1L$ at 0.2 K. The signal is approximately linear around c' at high temperature but deviates from linearity as field is increased. The deviation gets bigger as temperature is lowered. For the lowest temperature the $-1L$ data is highly nonlinear and appears to indicate an onset or threshold field. The Nernst signal is about zero for $B < 4$ T. It starts increasing at 4.2 T, then increases steeply after 6 T. (The highly nonlinear field dependence prevents us from plotting a Nernst coefficient.)

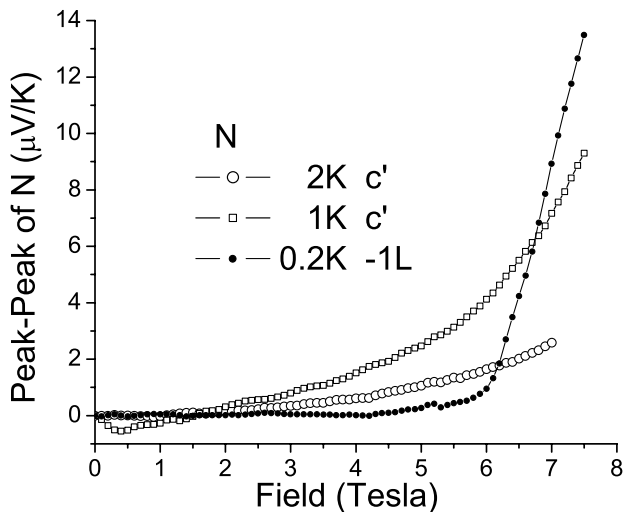


FIG. 3. Field dependence of peak-peak values of Nernst signal N at 2 and 1 K for c' and at 0.2 K for $-1L$. We obtained the peak-to-peak value by taking the difference of Nernst signals at the angles where we found the maximum/minimum.

What is most striking about our data is the large resonantlike structures as the field is rotated through a Lebed MA. The most straightforward and probably correct interpretation is that, when the field is close to a MA, the current flows at the MA. In more conventional systems, in very high magnetic field the current follows the field lines and does not cross them [18]. In the present case the current effectively “locks in” to the MA, which corresponds to an interchain direction. This behavior is cartooned in Fig. 4. If the current locks in, then the field makes an angle with the current when it “lags” the MA and there is a Lorentz force, which gives a Hall effect if it is electric current or Nernst effect if it is heat (entropy) current. Similarly, on the other side of the magic angle, when the field “leads” the MA, the Lorentz force, Hall effect, and Nernst change sign. At precisely the MA the current and field are parallel and the Lorentz force, Hall, and Nernst signal are zero. This argument strongly suggests that the current locks in to the MA-interchain direction and provides a qualitative way of estimating the shape and magnitude of the effect.

The Nernst effect is the voltage generated in the $\nabla T \times \mathbf{B}$ direction by an imposed thermal gradient and is usually “small.” In a simple Drude model for particles with mass m , charge q , 1 degree of freedom per carrier, density n , and scattering time τ , the conductivity is $\sigma = nq^2\tau/m$, the Hall coefficient is $R_H = 1/nq$, the thermopower $S_1 = k_B/q$, the magnetoresistance $\Delta R/R = 0$, and the Nernst coefficient $N = 0$. On the other hand, if we imagine a system with two oppositely charged but otherwise identical carriers, $\sigma = 2nq^2\tau/m$, $S = 0$, $R_H = 0$, $N = k_B\tau B/m = (k_B/q)(\omega_c\tau) = (S_1)(\omega_c\tau)$, and $\Delta R/R = (\omega_c\tau)^2$. Since most systems are neither single carrier, single mass, single scattering time, nor completely electron-hole symmetric, we should expect all coefficients to be nonzero and of a magnitude given by the simple expressions above. Thus, the Nernst coefficient should be of the order of $N \sim (S_1)(\omega_c\tau)$. For a metal $S_1 \sim (k_B/e)(T/T_F) \sim 4$ nV/K at 0.2 K for $(\text{TMTSF})_2\text{PF}_6$ in the metallic state [19]. The appropriate ω_c should involve the component of the applied field perpendicular to the MA so that the maximum observed Nernst coefficient at 7.5 T

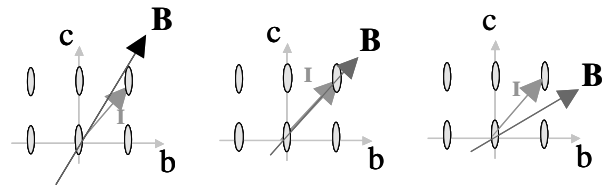


FIG. 4. Looking down the TMTSF chains. For the field near the $\mathbf{b} + \mathbf{c}$ direction the current flows only between the chains separated by $\mathbf{b} + \mathbf{c}$. The Lorentz force then produces a force along \mathbf{a} in the first figure, along $-\mathbf{a}$ in the last figure, and no force in the middle figure when the field and the current are parallel. Note that here we use an orthorhombic approximation.

should be of order 1 nV/K rather than the 10 μ V/K which is observed at that temperature.

In order to have a better understanding of the Nernst effect, we performed numerical calculations of a Boltzmann transport model based on Osada's model [9] for the Lebed MA effects. Osada's model assumes transfer integrals between several neighboring chains and can explain the existence of dips observed in magnetotransport for R_{zz} (transport along the least conducting direction) [20]. The numerical calculation can roughly reproduce the shape of the observed Nernst signal, but gives a magnitude that is about 5 orders of magnitude too low. Similarly, we can obtain the resonances but not the magnitude using an extension of the fitting scheme proposed by Ref. [21]. In the Boltzmann model, the Nernst effect is linear with temperature T at low temperature, also in contradiction with these experiments.

The giant value of the Nernst effect is not understood and appears difficult to explain in conventional Fermi liquid models. It may result from extremely correlated narrow bands as suggested by recent spectroscopic studies for these materials [4] once they are decoupled into 1D non-Fermi liquids or from something more exotic such as an interchain spinon drag [22].

In summary, we have observed giant resonantlike Nernst signals at MAs in $(\text{TMTSF})_2\text{PF}_6$ under 10 kbar pressure. This strongly suggests that the current is locked in to the Lebed MA directions for applied magnetic field close to the MAs. The transport between the quasi-one-dimensional TMTSF conducting chains is directly between neighboring chains close to the direction of the applied magnetic field (not in the imposed current/heat current direction nor in the direction of the applied field). For fields aligned along the MAs $(\text{TMTSF})_2\text{PF}_6$ may be a normal metal. For fields slightly away from the MAs the Nernst signal is several orders of magnitude larger than estimated from conventional Fermi liquid transport models, is highly nonlinear in the applied magnetic field, and is "nonmetallic" (increasing with decreasing temperature).

We acknowledge support from NSF DMR 9976576 and 9809483 and useful discussions with Phuan Ong, Phil Anderson, David Huse, and Iddo Ussishkin.

*Electronic address: wdu@princeton.edu

†Present address: Department of Physics, Chonbuk National University, Chonju, Korea, 561-756.

- [1] D. Jérôme, *et al.*, J. Phys. (Paris) Lett. **41**, L95 (1980).
- [2] For a review, please see T. Ishiguro, K. Yamaji, and G. Saito, *Organic Superconductors* (Springer, New York, 1998), 2nd ed.
- [3] I. J. Lee *et al.*, Phys. Rev. Lett. **88**, 017004 (2002); **78**, 3555 (1997).
- [4] V. Vescoli *et al.*, Science **281**, 1181 (1998).

- [5] T. Lorenz *et al.*, Nature (London) **418**, 614 (2002).
- [6] A. G. Lebed, JETP Lett. **43**, 174 (1986); A. G. Lebed and P. Bak, Phys. Rev. Lett. **63**, 1315 (1989).
- [7] T. Osada *et al.*, Phys. Rev. Lett. **66**, 1525 (1991); M. J. Naughton *et al.*, Phys. Rev. Lett. **67**, 3712 (1991); W. Kang *et al.*, Phys. Rev. Lett. **69**, 2827 (1992).
- [8] If $(\text{TMTSF})_2\text{PF}_6$ were orthorhombic, most treatments suggest that the "MAs" would correspond to magnetic fields aligned along $m\mathbf{b} + n\mathbf{c}$, where \mathbf{a} , \mathbf{b} , and \mathbf{c} are real space lattice vectors, and m and n are integers. However, $(\text{TMTSF})_2\text{PF}_6$ is triclinic with real space vectors \mathbf{a} , \mathbf{b} , and \mathbf{c} and reciprocal lattices \mathbf{a}^* , \mathbf{b}^* , and \mathbf{c}^* , e.g., $\mathbf{b}^* = \frac{2\pi\mathbf{c} \times \mathbf{a}}{\mathbf{a} \cdot (\mathbf{b} \times \mathbf{c})}$. In this and most previous papers, angular rotations are done in the $\mathbf{b}^*\mathbf{c}^*$ plane perpendicular to the \mathbf{a} axis. Commensurate orbits [6,9] then correspond to fields in the $\mathbf{b}^*\mathbf{c}^*$ plane, but along the directions $m\mathbf{b}' + n\mathbf{c}'$, with $\mathbf{b}' = \frac{2\pi\mathbf{c}^* \times \mathbf{a}}{\mathbf{a} \cdot (\mathbf{b}^* \times \mathbf{c}^*)}$ and $\mathbf{c}' = \frac{2\pi\mathbf{a} \times \mathbf{b}^*}{\mathbf{a} \cdot (\mathbf{b}^* \times \mathbf{c}^*)}$. For example, a Fermi surface orbit along the \mathbf{c}^* direction requires a field along $\mathbf{b}' \perp \mathbf{c}^*$. In real space these are directions between the highly conducting stacks of TMTSF molecules. Thus, other interpretations of the MA effect involve magnetic field dephasing of interchain hopping.
- [9] T. Osada *et al.*, Phys. Rev. B **46**, 1812 (1992); T. Osada, Physica (Amsterdam) **256B**, 633 (1998); T. Osada *et al.*, Synth. Met. **103**, 2024 (1999).
- [10] K. Maki, Phys. Rev. B **45**, 5111 (1992); V. M. Yakovenko, Phys. Rev. Lett. **68**, 3607 (1992); P. M. Chaikin, Phys. Rev. Lett. **69**, 2831 (1992); A. G. Lebed, J. Phys. I (France) **6**, 1819 (1996).
- [11] S. P. Strong *et al.*, Phys. Rev. Lett. **73**, 1007 (1994).
- [12] E. I. Chashechkina and P. M. Chaikin, Phys. Rev. Lett. **80**, 2181 (1998).
- [13] P. M. Chaikin *et al.*, Rev. Sci. Instrum. **52**, 1397 (1981).
- [14] R. C. Yu, Ph.D. dissertation, University of Pennsylvania, 1990 (unpublished).
- [15] L. Onsager, Phys. Rev. **37**, 405–426 (1931); **38**, 2265–2279 (1931).
- [16] W. Kang *et al.*, Phys. Rev. B **45**, 13566 (1992).
- [17] It is likely along the \mathbf{c}' axis based on our analysis.
- [18] For example, in a free electron gas system, under magnetic field the electrons all spiral along the field line with radii $r \leq mv_f/eB$. Here v_f is the Fermi velocity. In high field limit, the cyclotron orbits shrink, so, effectively, the electron can drift only along field lines, i.e., the current can flow only along the field lines.
- [19] The Fermi energy $E_F \sim 0.35$ eV ($T_F \sim 4000$ K), scattering time $\tau \sim 4.2 \times 10^{-12}$ sec at low T ; see Ref. [2].
- [20] Osada's model as well as several other microscopic models do not even qualitatively explain the shape of the angular dependence of R_{zz} for $(\text{TMTSF})_2\text{PF}_6$ or R_{xx} or R_{yy} for any of the Bechgaard salts.
- [21] E. I. Chashechkina and P. M. Chaikin, Phys. Rev. B **65**, 012405 (2002).
- [22] For example, an electron on a single chain may dissociate into a spinon and a holon. However, when moving to another chain it must tunnel as an electron. Once on the neighboring chain the spinon can again dissociate and regain its degrees of freedom and entropy/heat.